# Coupling conditions for the shallow water equations on a network

Jean-Guy Caputo, Denys Dutykh, Bernard Gleyse

Jean-Guy Caputo
*INSA de Rouen, France*

Denys Dutykh
*CNRS, Université Savoie Mont Blanc, France*

Bernard Gleyse
*INSA de Rouen, France*

# Coupling conditions for the shallow water equations on a network

arXiv.org / HAL

# COUPLING CONDITIONS FOR THE SHALLOW WATER EQUATIONS ON A NETWORK

JEAN-GUY CAPUTO*, DENYS DUTYKH, AND BERNARD GLEYSE

Abstract. We study numerically and analytically how nonlinear shallow water waves propagate in a fork. Using a homothetic reduction procedure, conservation laws and numerical analysis in a 2D domain, we obtain angle dependent coupling conditions for the water height and the velocity. We compare these to the ones for a class of scalar nonlinear wave equations for which the angle plays no role.

**Key words and phrases:** Networks; shallow water equations; nonlinear wave equations

**MSC:** [2010]35Qxx (primary)

* Corresponding author.

Contents

# 1. Introduction

To study the propagation of nonlinear waves in networks, a first step is to consider a simple fork as a model of elementary junctions. Another natural simplification is to reduce the problem from a 2D partial differential equation to a 1D effective partial differential equation with adequate coupling conditions at the interfaces. Recently [1], we introduced a homothetic reduction [4] where we average the operator over the fork region and consistently take the limit when the width tends to zero. For the sine-Gordon nonlinear wave equation, this gave the right interface conditions for the 1D model. The energy time plots for the 2D system and the 1D effective model agreed very well. The angle of the fork did not appear to play any significant role.

For classical hydrodynamics, the angle in the fork sets the forces experienced by the pipes [7]: it is then very important. When considering networks of rivers, many authors, for example Stoker [13] and Jacovkis [6] assume continuity of the water height and continuity of the flux so that the angle of the fork does not come in. Recently, Herty and Seaid [5] compared 2D solutions with solutions of a 1D effective model. They used damping in their equations and did not address the angle issue. While damping is important for applications, it breaks the conservative character of the equations. As for classical hydrodynamics, in shallow water flows, the angle is important; the energy entering a branch can vary from 20% to 50% depending on the angle of the branch with the main branch. It is then important to provide the 1D model with coupling conditions that reflect this dependence.

A few authors have addressed the problem. Schmidt [9] studied the 2D connection between 1D channels. No assumption is made on the size of the connecting domain. The flow in the junction is assumed linear. The authors use a variational method: the solution is taken as a superposition of fields. The final result is a system of ordinary differential equations for the values at the ends of the branches coupled to the shallow water PDEs. Despite its formal beauty it remains difficult to handle and does not give a simple picture. Another recent study by Nachbin and Simoes [8] on the dispersive shallow water equations transforms the fork into a rectangle with a cut using a conformal map. The 2D PDE in this rectangle is then averaged transversally to obtain a 1D model whose solutions agree remarkably well with the ones of the original 2D model for small fork angles. The 1D model also gives interface conditions, based on the averaged Jacobian of the transformation; these generalize the ones of Stoker. These coupling conditions work for small angles; they contain the angle dependance implicitly through the Jacobian of the conformal map.

In this article, using conservation laws, we get simple and explicit coupling conditions that depend on the angle. For that, we revisit the general problem using our homothetic reduction procedure. We consider a general class of scalar nonlinear wave equations, for example the 2D sine–Gordon equation or the 2D reaction-diffusion equation with homogeneous Neuman boundary conditions and the shallow water equations. For the first model, the reduction is natural and we obtain simple jump conditions : continuity of the field and continuity of the gradient (Kirchoff law). The angle of the channels does not play any role in the reduction and we obtain the same 1D effective model for any $n$ channel configuration,

confirming the results of [1]. For the shallow water equations, the reduction gives mass and energy couplings; the former is the flux conservation used by Stoker. The reduction of the momenta shows additional terms appearing; these contain the effect of the boundary and therefore the angular dependance. We illustrate this on a simple T fork geometry and input the wave on two different branches to analyze the angular dependence of the solution. Using the 2D numerical solution together with the results of the reduction, we obtain new explicit coupling conditions at the interface that depend on the angle configuration. These will give a consistent 1D effective model.

The article is organized as follows. After recalling the shallow water equations and their conserved quantities in Section 2, we present the geometries in Section 3. Section 4 shows the straightforward reduction of a general class of nonlinear wave equations. Section 5 presents the reduction for the shallow water equations; while the results are simple for the mass and the energy, they are complex for the momenta. A detailed analysis of the two main branch dynamical problems is presented in Section 6; there we give the new coupling conditions. Conclusions are given in Section 7.

## 2. The nonlinear shallow water equations

The shallow water equations in a 2D domain can be written in terms of the fluid velocity $\mathbf{u}(x,t)$

$$\mathbf{u} \;=\; (u,v)^T.$$

and the water height $h(x,t)$ [13]. They read

$$h_t \;+\; \nabla\cdot(h\mathbf{u}) \;=\; 0, \tag{2.1}$$

$$(hu)_t \;+\; \nabla\cdot\begin{pmatrix} hu^2+\frac{gh^2}{2} \\ huv \end{pmatrix} \;=\; 0, \tag{2.2}$$

$$(hv)_t \;+\; \nabla\cdot\begin{pmatrix} huv \\ hv^2+\frac{gh^2}{2} \end{pmatrix} \;=\; 0, \tag{2.3}$$

where $g$ is the gravity acceleration. The wall boundary condition is

$$\mathbf{u}\cdot\mathbf{n} \;=\; 0. \tag{2.4}$$

We assume an even bottom of the channels.

### 2.1. Conserved quantities

We can first recall the conserved quantities. Integrating equations (2.1)–(2.3) over a 2D closed domain $\Omega$ and using the boundary condition (2.4) we get

$$\partial_t \int_\Omega h \, \mathrm{d}x\mathrm{d}y = 0, \tag{2.5}$$

$$\partial_t \int_\Omega hu \, \mathrm{d}x\mathrm{d}y + \int_{\partial\Omega} \frac{gh^2}{2} n_x \, \mathrm{d}s = 0, \tag{2.6}$$

$$\partial_t \int_\Omega hv \, \mathrm{d}x\mathrm{d}y + \int_{\partial\Omega} \frac{gh^2}{2} n_y \, \mathrm{d}s = 0. \tag{2.7}$$

The first conserved quantity is the integral of the water elevation

$$M = \int_\Omega h \, \mathrm{d}x\mathrm{d}y.$$

The total $x$ and $y$ momenta

$$P_x = \int_\Omega (hu^2 + \frac{gh^2}{2}) \, \mathrm{d}x\mathrm{d}y, \quad P_y = \int_\Omega (hv^2 + \frac{gh^2}{2}) \, \mathrm{d}x\mathrm{d}y$$

are not conserved in the geometries that we will consider.

A flux relation that can be deduced from the conservation laws is the total energy flux where the total energy density is

$$e = \frac{1}{2}\left[gh^2 + (u^2 + v^2)h\right]. \tag{2.8}$$

From (2.1)–(2.3) it can be seen that

$$e_t + \nabla \cdot \left[\mathbf{u}(e + \frac{gh^2}{2})\right] = 0. \tag{2.9}$$

From this relation, one obtains the conservation of the energy $e$ for localized waves

$$E = \int_\Omega e \, \mathrm{d}x\mathrm{d}y.$$

## 3. The different geometries

To reduce the 2D problem to a 1D effective problem, we will proceed as in [1] and integrate the operators on the different subdomains corresponding to the defect. Then we will examine the behavior of the different terms as $w$, the width of the branches, goes to zero. It is then important that the domains that we consider behave in a regular way as we shrink $w$ to zero, [4]. We will have a consistent one-dimensional model if the limit is well defined.

### 3.1. The elbow

A first simple domain is the elbow shown in Fig. 1. The two branches have a width $w$. The defect region has two inside components $CA$ and $BC$ of length $w$. The other components $AB$ and $BE$ scale like $w$ as can be seen from the coordinates of $A$, $C$ and $B$.

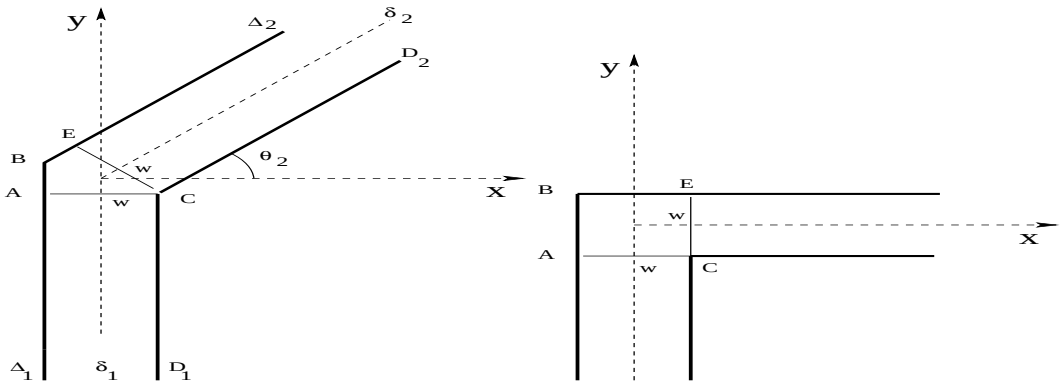


**Figure 1.** *A simple elbow geometry with an arbitrary angle (left) and a right angle (right).*

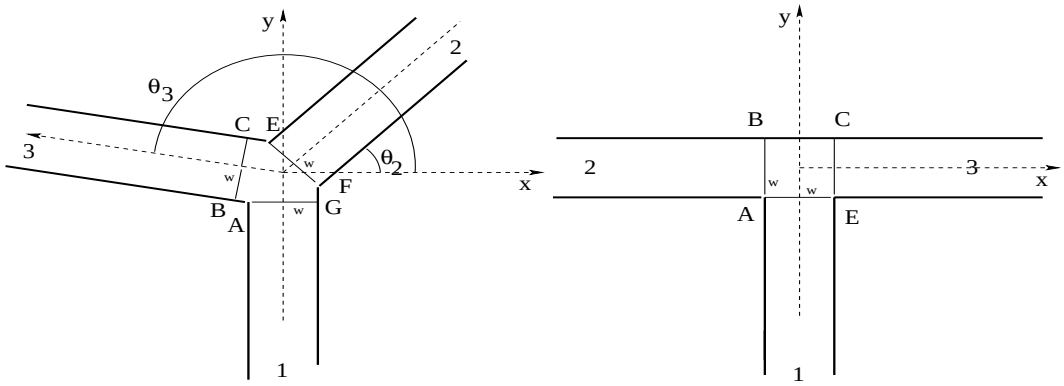


**Figure 2.** *A fork geometry with arbitrary angles (left) and with right angles (right).*

Then when $w \to 0$, the domain reduces to two lines. In Fig. 1 the left panel is a configuration with an arbitrary angle and the right panel shows the right angle configuration for which the calculations are easier.

## 3.2. The branch

The elbow is a simple configuration which shows how the angle influences the coupling conditions. However we are mostly interested in branches or forks as in Fig. 2. As for the elbow, these domains reduce to lines when $w \to 0$. We will concentrate on the right angle domain (right panel of Fig. 2). The calculations for a general domain (right panel of Fig. 2) can be generalized in a straightforward way.

## 4. Reduction for a class of scalar nonlinear wave equations

Before giving the results for the shallow water equations, we analyze the simpler case of a class of scalar nonlinear wave equations. The 2D nonlinear wave equation that we consider is a large class that includes hyperbolic wave equations like the sine-Gordon equation as well as reaction diffusion equations like the Fisher equation. It can be written

$$\alpha u_{tt} + \beta u_t - \Delta u = N(u), \tag{4.1}$$

where $u(x,y,t)$ is a scalar, $\Delta$ is the usual 2D Laplacian and where $N(u)$ is a nonlinearity that does not contain derivatives. The boundary condition is of Neuman type

$$\partial_n u = grad(u)\cdot \mathbf{n} = 0. \tag{4.2}$$

The reduction of this class of scalar nonlinear wave equations is much simpler than the one of the shallow water equations. In all cases we get an effective 1D model. To illustrate this consider the asymmetric Y-branch. A first assumption is the continuity of $u$ which is obvious for the 2D operator. The other condition comes from the integration of the operator (4.1) on the fork domain. We get

$$\int \left[\alpha u_{tt} + \beta u_t - N(u)\right] \mathrm{d}x\mathrm{d}y - \int_{ABCEFGA} (\nabla u)\cdot \mathbf{n}\, \mathrm{d}s = 0.$$

The first integral is of order $\mathcal{O}(w^2)$. On the exterior boundaries, $(\nabla u)\cdot \mathbf{n} = 0$ so the line integral reduces to

$$\int_{BC} \cdots + \int_{EF} \cdots + \int_{AG} \cdots$$

which are $\mathcal{O}(w)$. We then obtain for $w \to 0$

$$-\partial_s u_1 + \partial_s u_2 + \partial_s u_3 = 0, \tag{4.3}$$

where $u_i$, $i = 1,2,3$ are respectively the values of the field at the end of branch 1 $(AC)$ and at the beginning of branch 2 $(CE)$. Relation (4.3) is Kirchhoff's law [1]. In this case the angle does not play a role. These results were confirmed numerically in [1], we do not present them here.

When the widths of the branches are not equal, the Kirchoff relation becomes

$$-w_1\partial_s u_1 + w_2\partial_s u_2 + w_3\partial_s u_3 = 0. \tag{4.4}$$

## 5. Reduction of the shallow water equations

The shallow water equations cannot be reduced so simply as the nonlinear scalar wave equation. In fact, it is not clear what are the right interface conditions that should be implemented for a 1D effective model.

To understand the problem, we proceed as in [1], integrate the operator on the bifurcation region and consider the limit of small transverse width $w$. We consider first the elbow geometry and give all the details for this relatively simple case. The calculations for the other geometries can be obtained in a similar way.

## 5.1. Mass flux

Integrating the equation (2.1) over the region $CABEC$ yields

$$\int_{CABEC} h_t \, \mathrm{d}x\mathrm{d}y \; + \; \int_{CABEC} h \; \mathbf{u}\cdot\mathbf{n} \, \mathrm{d}s \; = \; 0.$$

Because of the boundary condition $\mathbf{u}\cdot\mathbf{n} \; = \; 0$ on $ABE$, the expression above reduces to

$$\int_{CABEC} h_t \, \mathrm{d}x\mathrm{d}y \; + \; \int_{CA} h \; \mathbf{u}\cdot\mathbf{n} \, \mathrm{d}s \; + \; \int_{EC} h \; \mathbf{u}\cdot\mathbf{n} \, \mathrm{d}s \; = \; 0.$$

The first integral is $\mathcal{O}(w^2)$ while the two other integrals are $\mathcal{O}(w)$. Dividing the equation by $w$ and taking the limit $w \to 0$ we get from these two terms

$$-\, h_1 u_1^{\parallel} \; + \; h_2 u_2^{\parallel} \; = \; 0. \tag{5.1}$$

where we have introduced the local branch-oriented velocities $u^{\parallel}, u^{\perp}$ and the indices 1 and 2 refer to the branches. Of course, when the transverse widths $w_1$, $w_2$ are different, with the condition that the ratio $w_2/w_1$ remains finite, the relation (5.1) becomes

$$-w_1 h_1 u_1^{\parallel} \; + \; w_2 h_2 u_2^{\parallel} \; = \; 0$$

The generalization of (5.1) to the fork $ABCEFGA$ is standard, it is

$$-\, h_1 u_1^{\parallel} \; + \; h_2 u_2^{\parallel} \; + \; h_3 u_3^{\parallel} \; = \; 0. \tag{5.2}$$

## 5.2. Energy flux

The energy flux (2.9) can be consistently reduced to a 1D relation. To see this, let us consider again the elbow geometry for simplicity. We integrate equation (2.8) over the region $CABEC$ to obtain

$$\int_{CABEC} e_t \, \mathrm{d}x\mathrm{d}y \; + \; \int_{CABEC} (e + \frac{gh^2}{2}) \; \mathbf{u}\cdot\mathbf{n} \, \mathrm{d}s \; = \; 0.$$

Because of the boundary condition $\mathbf{u}\cdot\mathbf{n} = 0$ on $ABE$, the expression above reduces to

$$\int_{CABEC} e_t \, \mathrm{d}x\mathrm{d}y \; + \; \int_{CA} (e + \frac{gh^2}{2}) \; \mathbf{u}\cdot\mathbf{n} \, \mathrm{d}s \; + \; \int_{EC} (e + \frac{gh^2}{2}) \; \mathbf{u}\cdot\mathbf{n} \, \mathrm{d}s \; = \; 0.$$

The first integral is $\mathcal{O}(w^2)$ while the two other integrals are $\mathcal{O}(w)$. Dividing the equation by $w$ and taking the limit $w \to 0$ we get from these two terms

$$-\, (e_1 + \frac{gh_1^2}{2}) u_1^{\parallel} \; + \; (e_2 + \frac{gh_2^2}{2}) u_2^{\parallel} \; = \; 0. \tag{5.3}$$

As above, we generalize this relation to the fork geometry and get

$$-\, (e_1 + \frac{gh_1^2}{2}) u_1^{\parallel} \; + \; (e_2 + \frac{gh_2^2}{2}) u_2^{\parallel} \; + \; (e_3 + \frac{gh_3^2}{2}) u_3^{\parallel} \; = \; 0. \tag{5.4}$$

To conclude, equation (2.1) gives in the 1D limit, the conservation of mass (5.2). The same happens for the energy flux (2.9) which yields (5.4). The natural matching conditions

for 1D shallow water equations on a network are then

$$-h_1 u_1^{\parallel} \;-\; h_2 u_2^{\parallel} \;+\; h_3 u_3^{\parallel} \;=\; 0, \tag{5.5}$$

$$-u_1^{\parallel}(gh_1^2 + \frac{{u_1^{\parallel}}^2}{2}) \;-\; u_2^{\parallel}(gh_2^2 + \frac{{u_2^{\parallel}}^2}{2}) \;+\; u_3^{\parallel}(gh_3^2 + \frac{{u_3^{\parallel}}^2}{2}) \;=\; 0. \tag{5.6}$$

Note that the angles of the fork do not play any role. This is a similar situation to the one of the nonlinear scalar wave equation.

## 5.3. Momentum flux

Contrary to the mass and the energy, the momentum equations (2.2)–(2.3) cannot be consistently reduced to a 1D condition. A first observation is that the two components of the momentum are generally not conserved in a bifurcation or a fork. We illustrate this for the $T$ geometry (right panel of Fig. 2) because the calculations are simpler; nevertheless, this configuration yields all the features of the problem.

Integrating equation (2.2) yields

$$\int (hu)_t \,\mathrm{d}x\mathrm{d}y \;+\; \int_{ABCEA} \begin{pmatrix} hu^2 + \frac{gh^2}{2} \\ huv \end{pmatrix} \cdot \mathbf{n} \,\mathrm{d}s \;=\; 0.$$

The first term is $O(w^2)$. Keeping only the $O(w)$ terms (line integrals) we get

$$\int_{AB} \begin{pmatrix} hu^2 + \frac{gh^2}{2} \\ huv \end{pmatrix} \cdot \begin{pmatrix} -1 \\ 0 \end{pmatrix} \mathrm{d}s \;+\; \int_{BC} \begin{pmatrix} hu^2 + \frac{gh^2}{2} \\ huv \end{pmatrix} \cdot \begin{pmatrix} 0 \\ 1 \end{pmatrix} \mathrm{d}s$$
$$+ \int_{CE} \begin{pmatrix} hu^2 + \frac{gh^2}{2} \\ huv \end{pmatrix} \cdot \begin{pmatrix} 1 \\ 0 \end{pmatrix} \mathrm{d}s \;+\; \int_{EA} \begin{pmatrix} hu^2 + \frac{gh^2}{2} \\ huv \end{pmatrix} \cdot \begin{pmatrix} 0 \\ -1 \end{pmatrix} \mathrm{d}s \;=\; 0.$$

We then get

$$-\,h_1 u_1 v_1 \;-\; (h_2 u_2^2 + g\frac{h_2^2}{2}) \;+\; h_3 u_3^2 + g\frac{h_3^2}{2} \;=\; 0. \tag{5.7}$$

Similarly for the $y$ momentum, we get

$$\int_{AB} \begin{pmatrix} huv \\ hv^2 + \frac{gh^2}{2} \end{pmatrix} \cdot \begin{pmatrix} -1 \\ 0 \end{pmatrix} \mathrm{d}s \;+\; \int_{BC} \begin{pmatrix} huv \\ hv^2 + \frac{gh^2}{2} \end{pmatrix} \cdot \begin{pmatrix} 0 \\ 1 \end{pmatrix} \mathrm{d}s$$
$$+ \int_{CE} \begin{pmatrix} huv \\ hv^2 + \frac{gh^2}{2} \end{pmatrix} \cdot \begin{pmatrix} 1 \\ 0 \end{pmatrix} \mathrm{d}s \;+\; \int_{EA} \begin{pmatrix} huv \\ hv^2 + \frac{gh^2}{2} \end{pmatrix} \cdot \begin{pmatrix} 0 \\ -1 \end{pmatrix} \mathrm{d}s \;=\; 0.$$

This gives

$$-\,h_1 v_1^2 \;+\; g\frac{h_1^2}{2} \;-\; h_2 u_2 v_2 \;+\; g\frac{h_{23}^2}{2} \;+\; h_3 u_3 v_3 \;=\; 0, \tag{5.8}$$

where the term $h_{23}$ is an unknown value, which can be obtained by interpolation of $h_2$ and $h_3$; it represents the field $h$ on the side $BC$. The terms $u_1$, $v_2$, $v_3$ disappear in the limit $w \to 0$ so the final results are

$$h_2 u_2^2 \;+\; g\frac{h_2^2}{2} \;+\; h_3 u_3^2 \;+\; g\frac{h_3^2}{2} \;=\; 0. \tag{5.9}$$

$$-h_1 v_1^2 + g\frac{h_1^2}{2} + g\frac{h_{23}^2}{2} = 0. \tag{5.10}$$

Contrary to the mass and energy which give clear jump conditions in the 1D limit (5.5), the relations for the momentum involve extra terms which need to be approximated. To understand how to proceed, we have solved numerically the 2D shallow water equations.

## 6. Numerical method for solving the 2D shallow water equations

For simplicity we concentrate on the $T$ geometry. To solve the equations (2.1)–(2.3), we choose as space unit the depth $d$. The time unit is then $\sqrt{\frac{d}{g}}$. The variables and fields are then rescaled as

$$x' = \frac{x}{d}, \quad t' = t\sqrt{\frac{g}{d}}, \quad h' = \frac{x}{d}, \quad u' = \frac{u}{\sqrt{gd}}. \tag{6.1}$$

This amounts to taking $d = 1$, $g = 1$ in (2.1)–(2.3).

We solve the nonlinear shallow water equations using a first order finite volume scheme on an unstructured triangular mesh (produced with the Gmsh software). This scheme is explained in detail in [3]. The typical size of the triangles is 0.02. For the time integration we use a variable order Adams–Bashforth–Moulton multistep solver (implemented in Matlab under `ode113` subroutine [12]). The relative and absolute tolerances were set to $10^{-5}$.

The initial condition is taken as a traveling solitary wave of velocity $c$. This is an exact solution for the mass conservation law. We use a solitary wave inspired from the Serre's solitary wave solution [10, 11]. See [2] for the exact formula.

$$h(x, y, t = 0) = d + a\,\mathrm{sech}^2\left(\tfrac{1}{2}k(y - y_0)\right) \equiv d + \eta(x, y, 0), \tag{6.2}$$

$$v(x, y, t = 0) = c\frac{\eta(x)}{d + \eta(x)}, \tag{6.3}$$

where the speed is $c = \sqrt{g(d + a)}$. The other parameters in are

$$g = 1, \quad k = 2, \quad d = 1, \quad a = 1, \quad x_0 = y_0 = 2.5.$$

The calculations were done for three different values of the width $w$, $w = 0.5$, 0.25 and 0.125. The results are similar for these three values so that we will only present the results for $w = 0.125$.

The four equations obtained from integrating the operators for the mass, momentum and energy on the fork domain $ABCEA$ reduce to

$$\delta m \equiv -h_1 v_1 - h_2 u_2 + h_3 u_3 = 0, \tag{6.4}$$

$$\delta p_x \equiv -\left(h_2 u_2^2 + g\tfrac{h_2^2}{2}\right) + h_3 u_3^2 + g\tfrac{h_3^2}{2} = 0, \tag{6.5}$$

$$\delta p_y \equiv -\left(h_1 v_1^2 + g\tfrac{h_1^2}{2}\right) + g\tfrac{h_{23}^2}{2} = 0, \tag{6.6}$$

$$\delta e \equiv -v_1(gh_1^2 + \tfrac{v_1^2}{2}) - u_2(gh_2^2 + \tfrac{u_2^2}{2}) + u_3(gh_3^2 + \tfrac{u_3^2}{2}) = 0, \tag{6.7}$$

| *Type* | *known* | *unknown* |
|---|---|---|
| wave in branch 1 | $h_1, v_1$ | $h_2, u_2, h_3, u_3$ |
| wave in branch 3 | $h_3, u_3$ | $h_1, v_1, h_2, u_2$ |

**Table 1.** *The two different dynamic problems for the T branch.*

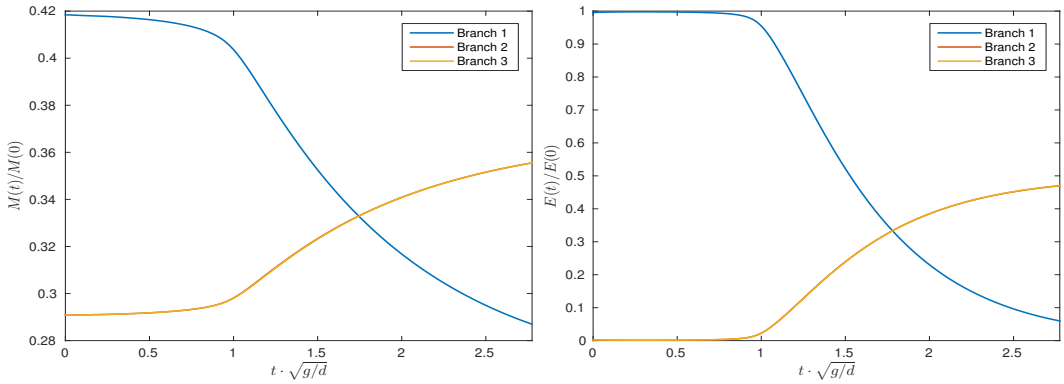


**Figure 3.** *Time evolution of the wave mass $M_w$ (left) and the wave energy $E_w$ (right) for a wave incident in branch 1.*

where we introduced the residuals $\delta m$, $\delta p_x$, $\delta p_y$ and $\delta e$. Two problems will be considered, whether we send the wave into branch 1 or branch 3. In these two problems, the number of unknowns is the same; see Table 1.

The wave mass and wave energy in each branch have been calculated. They are defined as

$$M_w = \int_\Omega (h-d)\ \mathrm{d}x\mathrm{d}y,$$

$$E_w = \int_\Omega \frac{1}{2}\left[g(h-d)^2 + (u^2+v^2)h\right]\ \mathrm{d}x\mathrm{d}y.$$

Energy will propagate very differently in problems 1 and 2. In the next sections we examine in detail the two types of problems and use the conservation laws to establish jump conditions for the 1D effective model.

## 6.1. Wave incident into branch 1

In this case, the wave in branch 1 will split up evenly between branches 2 and 3 which will receive 50% of the energy. This is apparent on the right panel of Fig. 3. The wave mass goes from 0.42 in branch 1 to 0.35 in branches 2 and 3; the total mass is conserved so we have

$$0.42 - 0.28 = 0.14 = 2 \times (0.35 - 0.28).$$

There is very little reflection for the wave amplitude we have considered, $a = 1$. For larger amplitudes, we enter the shock regime and there we observe a significant reflection.

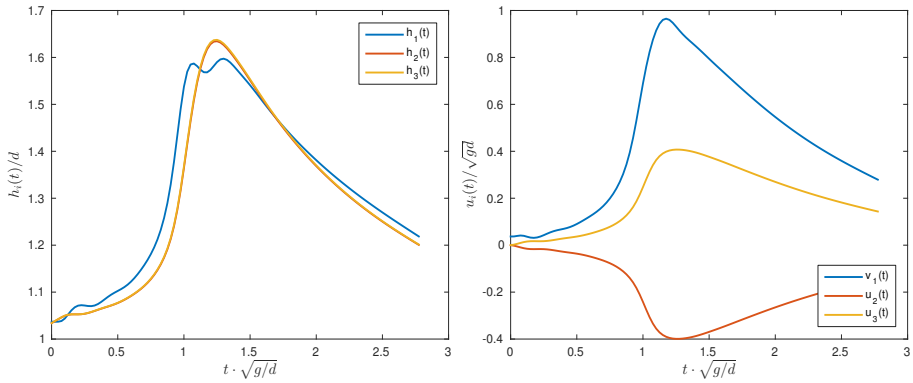


**Figure 4.** *Time evolution of the wave heights $h_1, h_2, h_3$ (left) and the wave speeds $v_1, u_2, u_3$ for a wave incident in branch 3.*

| *time* | $\delta m/M$ | $\delta e/E$ |
|---|---|---|
| 0.75 | -0.03 | -0.03 |
| 1 | -0.226 | -0.37 |
| 1.25 | -0.096 | -0.23 |
| 1.5 | -0.04 | -0.13 |
| 1.8 | -0.02 | -0.07 |
| 2.5 | -0.004 | -0.015 |

**Table 2.** *The mass and energy residuals $\delta m$, $\delta e$ in the equations (6.4)–(6.7) for different times.*

To verify the approximation given by the relations (6.4)–(6.7), we first computed the time evolution of the quantities $h_1$, $h_2$, $h_3$, $v_1$, $u_2$, $u_3$ from the 2D direct numerical simulations. We used a scattered linear interpolation to estimate the physical variables along the four different segments of the fork region from the unstructured triangular mesh data. The results are presented in Fig. 4.

The correspondence between the 2D solution and the 1D effective solution is summarized in the Table 2. There we report the values of the left hand sides in the equations (6.4)–(6.7) for the mass and the energy. These have been normalized by the initial mass and initial energy which are respectively

$$M = 1.77, \quad E = 2.37.$$

These results show that our approximation is valid most of the time except for the transient regime when the wave hits the wall. At that instant, the motion is significantly two dimensional so that an averaging procedure fails to capture the dynamics.

If we neglect the time instants when the 1D approximation breaks down, we can obtain interface conditions from (6.4)–(6.7). For that, we assume symmetry

$$h_2 = h_3, \qquad u_2 = -u_3.$$

We then get the two equations

$$h_2 u_2 = -\frac{1}{2} h_1 v_1, \tag{6.8}$$

$$2u_2\left(gh_2 + u_2^2\right) = -\frac{v_1}{2}\left(gh_1^2 + \frac{v_1^2}{2}\right). \tag{6.9}$$

The system reduces to the fourth degree equation

$$u_2{}^4 + pu_2 - q = 0, \tag{6.10}$$

where

$$p = \frac{v_1}{2}\left(gh_1^2 + \frac{v_1^2}{2}\right), \quad q = \frac{(h_1 v_1)^2}{2}.$$

The function

$$f(x) = x^4 + px - q$$

has a minimum at $x_m = -(p/4)^{\frac{1}{3}}$. It is such that $f(0) = -q < 0$ and $f(x_m) = -(p/4)^{\frac{1}{3}}\frac{3}{4}p - q < 0$. Therefore, there is always a negative root which solves approximately

$$x^4 + px = 0,$$

so that

$$x = -p^{\frac{1}{3}}.$$

This yields the jump conditions

$$h_2 = h_3 = -\frac{h_1 v_1}{2u_2}, \tag{6.11}$$

$$u_2 = -u_3 = -\left[\frac{v_1}{2}(gh_1^2 + \frac{v_1^2}{2})\right]^{\frac{1}{3}}. \tag{6.12}$$

## 6.2. Wave incident into branch 3

For this configuration, about 80% will continue in branch 2 and 20% will enter branch 1, as shown in the right panel of Fig. 5. This ratio varies with the wave amplitude. For larger amplitudes, almost 100% passes into branch 2. This confirms that that there is a strong angular dependence of the energy flow through the fork. The left panel shows the wave mass, 0.38 for branch 2, 0.34 for branch 1. Again the mass is conserved because

$$0.42 - 0.28 = 0.14 = (0.38 - 0.28) - (0.34 - 0.28).$$

When the wave is coming from branch 3, an obvious solution is

$$v_1 = 0, \quad u_2 = u_3, \quad h_2 = h_3, \quad h_1 = h_2. \tag{6.13}$$

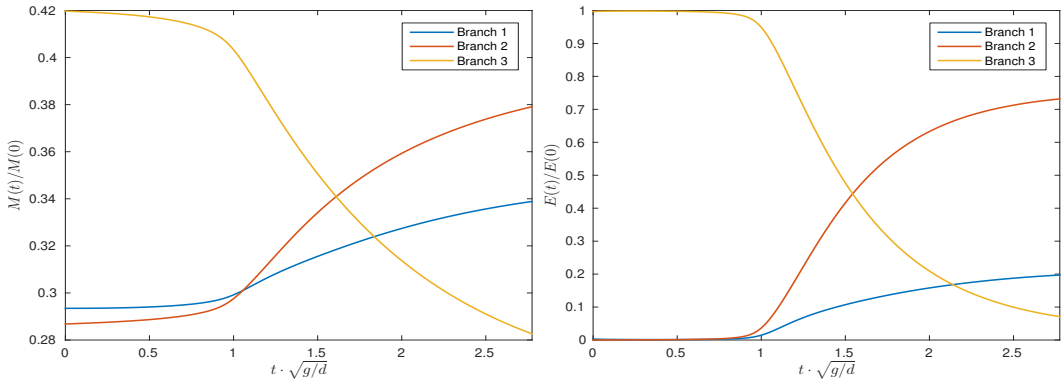


**Figure 5.** *Time evolution of the wave mass $M_w$ (left) and the wave energy $E_w$ (right) for a wave incident in branch* 3.

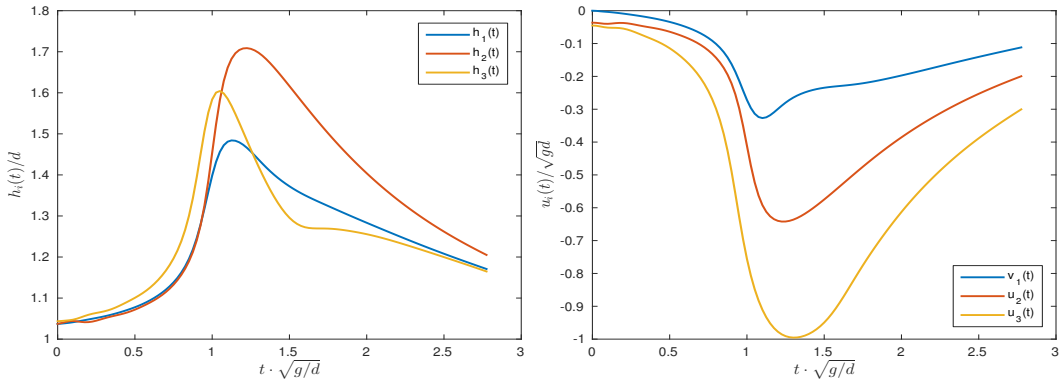


**Figure 6.** *Time evolution of the wave heights $h_1$, $h_2$, $h_3$ (left) and the wave speeds $v_1$, $u_2$ , $u_3$ for a wave incident in branch* 3.

This is simplistic, in reality $v_1 \neq 0$ but remains small. As for problem 1, to understand this, we compute the time evolution of the quantities $h_1$, $h_2$, $h_3$, $v_1$, $u_2$, $u_3$ from the 2D direct numerical simulations. Here about 20% of the energy is transferred to branch 1. The results are presented in Fig. 6.

The quantity

$$h_{23}^2 \equiv \frac{1}{w}\int_{BC} h^2 \, \mathrm{d}s, \tag{6.14}$$

in the $y$ component of the momentum is computed from the numerical solution. It is plotted as a function of time together with the estimate

$$h_{23}^2 \approx \frac{1}{2}(h_2^2 + h_3^2),$$

in Fig. 7. As can be seen, the agreement is very good.

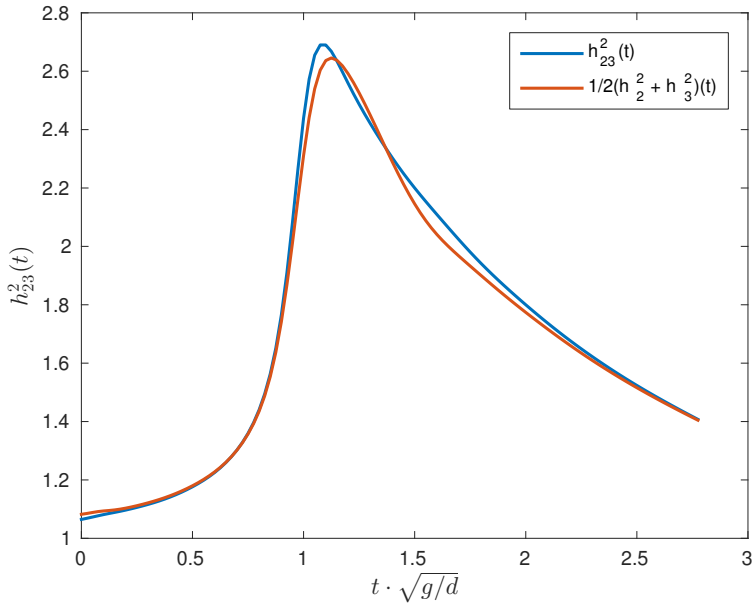


**Figure 7.** *Time evolution of the quantity* $h_{23}^2$ *from* (6.14) *together with* $\frac{1}{2}(h_2^2 + h_3^2)$.

| *time* | $\delta m/M$ | $\delta p_x/P_x$ | $\delta p_y/P_y$ | $\delta e/E$ |
|---|---|---|---|---|
| 0.75 | -0.03 | 0.10 | 0.02 | -0.04 |
| 1 | -0.12 | 0.66 | 0.06 | -0.27 |
| 1.25 | 0.02 | 0.28 | 0.08 | -0.009 |
| 1.5 | 0.002 | 0.14 | 0.06 | -0.003 |
| 1.8 | 0.02 | 0.07 | 0.01 | 0.02 |
| 2.5 | 0.01 | 0.02 | 0.001 | 0.008 |

**Table 3.** *The mass, momentum and energy residuals* $\delta m$, $\delta e$ *in the equations* (6.4)–(6.7) *for different times.*

The correspondence between the 2D solution and the 1D effective solution is summarized in the Table 3. There we report the values of $\delta m$, $\delta p_x$, $\delta p_y$ and $\delta e$ from equations (6.4)–(6.7). These have been normalized by the initial mass, momenta and energy which are respectively

$$M = 1.77, \quad P_x = 1.28, \quad P_y = 1.02, \quad E = 2.37.$$

Table 3 shows that the relations (6.4)–(6.7) hold well except at $t = 1$ and $t = 1.25$ for the $x$ momentum and energy.

Let us now extract the coupling conditions from the relations (6.4)–(6.7). As mentioned above, a naturally small parameter is $v_1$; $h_2$ can be considered large. Then from (6.5) we

get

$$h_1^2 = \frac{h_2^2 + h_3^2}{2}, \tag{6.15}$$

then, from (6.4)

$$v_1 = \frac{h_3 u_3 - h_2 u_2}{h_1}. \tag{6.16}$$

From (6.6) we get, neglecting the term $h_2 u_2^2$

$$\frac{g h_2^2}{2} = h_3 u_3^2 + \frac{g h_3^2}{2}, \tag{6.17}$$

which yields $h_2$. The velocity $u_2$ is given by the energy equation (6.7)

$$u_2 = \frac{u_3}{g h_2^2}\left(g h_3^2 + \frac{u_3^2}{2}\right). \tag{6.18}$$

To summarize, the coupling conditions are

$$h_2 = \sqrt{\frac{2}{g}\left(h_3 u_3^2 + \frac{g h_3^2}{2}\right)}, \qquad h_1 = \sqrt{\frac{h_2^2 + h_3^2}{2}}, \tag{6.19}$$

$$u_2 = \frac{u_3}{g h_2^2}\left(g h_3^2 + \frac{u_3^2}{2}\right), \qquad v_1 = \frac{h_3 u_3 - h_2 u_2}{h_1}. \tag{6.20}$$

## 7. Conclusion

We have studied the propagation of waves in a fork systematically using an homothetic reduction procedure that gives coupling conditions at the interface for an effective 1D PDE.

A nonlinear scalar wave equation like the 2D sine-Gordon or the 2D reaction diffusion equation naturally reduces to a 1D effective model. The coupling conditions are (i) continuity of the solution and (ii) continuity of the gradient (Kirchoff law). For these equations, the angle of the 2D branch is irrelevant, it does not affect the dynamics and there is always 50% of the energy that is transmitted to each branch. This is apparent in the 1D effective model.

For the nonlinear shallow water equations the angle of the branches is very important as shown in the simulations for the $T$ branch. We considered the 2D numerical solution and our reduction of the mass, momentum and energy laws on the fork region. The mass law gives the Stoker flux conservation. The momenta and energy laws can be used to derive the water height and velocity in the branches; these are the coupling conditions that should be used in a 1D effective model. They came naturally from the conservative nature of the shallow water equations.

The T geometry that we considered yielded an interesting side result. In the sub-critical regime, a wave coming from branch 1 will split into branches 2 and 3. In that sense, the shallow water solutions are "flexible". They are similar to sine-Gordon kinks that can excite transverse Fourier modes. In the super-critical regime, the shock wave stops at the

intersection: it needs to conserve its $y$ momentum and there is no way to do so except return back.

## Acknowledgments

The authors thank Tim Minzoni from UNAM Mexico for useful discussions. D. Dutykh would like to acknowledge the support from CNRS under the PEPS InPhyNiTi project "FARA".

## References

[1] J.-G. Caputo and D. Dutykh. Nonlinear waves in networks: model reduction for sine-Gordon. *Phys. Rev. E*, 90:022912, 2014. 4, 5, 6, 8

[2] D. Dutykh, D. Clamond, P. Milewski, and D. Mitsotakis. Finite volume and pseudo-spectral schemes for the fully nonlinear 1D Serre equations. *Eur. J. Appl. Math.*, 24(05):761–787, 2013. 11

[3] D. Dutykh, R. Poncet, and F. Dias. The VOLNA code for the numerical modeling of tsunami waves: Generation, propagation and inundation. *Eur. J. Mech. B/Fluids*, 30(6):598–615, 2011. 11

[4] J. Hadamard. *Leçons sur la géométrie élémentaire*. Librairie Armand Colin, Paris, 1906. 4, 6

[5] M. Herty and M. Seaïd. Assessment of coupling conditions in water way intersections. *Int. J. Num. Meth. Fluids*, 71(11):1438–1460, Apr. 2013. 4

[6] P. M. Jacovkis. One-Dimensional Hydrodynamic Flow in Complex Networks and Some Generalizations. *SIAM J. Appl. Math*, 51(4):948–966, 1991. 4

[7] L. D. Landau and E. M. Lifshitz. *Fluid Mechanics*. Pergamon Press, Oxford, 2nd edition, 1987. 4

[8] A. Nachbin and V. S. Simões. Solitary waves in forked channel regions. *J. Fluid Mech.*, 777:544–568, Aug. 2015. 4

[9] E. G. Schmidt. On Junctions in a Network of Canals. In O. Imanuvilov, G. Leugering, R. Triggiani, and B.-Y. Zhang, editors, *Control Theory of Partial Differential Equations*, pages 207–212. Chapman & Hall/CRC, Boca Raton, FL, 2005. 4

[10] F. Serre. Contribution à l'étude des écoulements permanents et variables dans les canaux. *La Houille blanche*, 8:374–388, 1953. 11

[11] F. Serre. Contribution à l'étude des écoulements permanents et variables dans les canaux. *La Houille blanche*, 8:830–872, 1953. 11

[12] L. F. Shampine and M. W. Reichelt. The MATLAB ODE Suite. *SIAM Journal on Scientific Computing*, 18:1–22, 1997. 11

[13] J. J. Stoker. *Water Waves: The Mathematical Theory with Applications*. John Wiley & Sons, Inc., Hoboken, NJ, USA, Jan. 1992. 4, 5

Laboratoire de Mathématiques, INSA de Rouen, BP 8, Avenue de l'Université, Saint-Etienne du Rouvray, 76801 France
*E-mail address*: caputo@insa-rouen.fr
*URL*: https://sites.google.com/site/jeanguycaputo/

LAMA, UMR 5127 CNRS, Université Savoie Mont Blanc, Campus Scientifique, 73376 Le Bourget-du-Lac Cedex, France
*E-mail address*: Denys.Dutykh@univ-savoie.fr
*URL*: http://www.lama.univ-savoie.fr/~dutykh/

Laboratoire de Mathématiques, INSA de Rouen, BP 8, Avenue de l'Université, Saint-Etienne du Rouvray, 76801 France
*E-mail address*: gleyse@insa-rouen.fr